

band model for GeTe and SnTe, assuming that the most significant couplings between bands are a transverse momentum coupling between the principal valence and conduction bands and a longitudinal coupling between the principal conduction and the second valence bands, we are able to explain most of the available experimental results for GeTe and SnTe.

#### ACKNOWLEDGMENTS

We are grateful to P. J. Stiles for his many helpful suggestions, D. O'Kane for supplying us the single-crystal GeTe and SnTe, J. Angilello for the x-ray work, and T. Hajos and J. Cummings for part of the optical and galvanomagnetic measurements.

### Optical Properties of VO<sub>2</sub> between 0.25 and 5 eV

HANS W. VERLEUR, A. S. BARKER, JR., AND C. N. BERGLUND

*Bell Telephone Laboratories, Murray Hill, New Jersey 07971*

(Received 5 April 1968)

The optical constants of VO<sub>2</sub> have been determined between 0.25 and 5 eV both below and above the semiconductor-metal transition temperature  $T_t=340^\circ\text{K}$ . Reflectivity and transmission spectra have been measured on both single crystals and thin films. The reflectivity spectra of the bulk crystals were measured with  $\mathbf{E}\perp$  ( $c$  axis) in the tetragonal phase [or  $\perp$  ( $a$  axis) in the monoclinic phase], and with  $\mathbf{E}$  parallel to these axes. While there are some differences in magnitude between the dielectric constants obtained from thin-film and single-crystal measurements, the structural features are in good agreement. Below  $T_t$  there are four prominent absorption peaks centered near photon energies of 0.85, 1.3, 2.8, and 3.6 eV. Above  $T_t$ , metallic free-carrier absorption is observed below 2.0 eV, but the same two absorption peaks near 3 and 4 eV are present. The energy location and polarization dependence of these two higher energy peaks can be related to similar absorption peaks in rutile, and are interpreted using the rutile band structure. The results are consistent with a picture in which filled bands arising primarily from oxygen  $2p$  orbitals are separated by approximately 2.5 eV from partially filled bands arising primarily from vanadium  $3d$  orbitals. Transitions from the filled  $2p$  bands are responsible for the high-energy peaks in the optical absorption in both the high- and low-temperature phases. In the high-temperature metallic phase, there is evidence that there is overlap among the  $3d$  bands such that at least two bands are partially occupied by the extra  $d$  electron per vanadium ion. In the low-temperature semiconductor phase, a band gap of approximately 0.6 eV opens up within the  $3d$  bands, separating two filled bands from higher-lying empty bands. The two absorption peaks at 0.85 and 1.3 eV are due to transitions from these two filled bands.

#### 1. INTRODUCTION

IT has been shown that VO<sub>2</sub> is one of several transition-metal oxides which show an abrupt change in some physical property such as electrical resistance or magnetic susceptibility at a temperature  $T_t$ .<sup>1,2</sup> In VO<sub>2</sub> the transition is probably best described as a first-order semiconductor-to-metal transition accompanied by a lattice distortion with  $T_t=68^\circ\text{C}$ . While no theory has yet been developed which predicts the transition temperature in VO<sub>2</sub>, recent work with idealized models pictures the transition as being of electronic origin.<sup>2,3</sup> The models suggest that above  $T_t$  the extra  $3d$  electron derived from each V<sup>4+</sup> ion resides in a partially filled  $d$  band giving metallic conduction. As the temperature is lowered it becomes energetically favorable for the crystal structure to change from tetragonal to monoclinic and for an energy gap to appear. Thus, below  $T_t$  VO<sub>2</sub> has a distorted structure, with a filled band separated by a gap from an empty band.

In this paper the optical properties of VO<sub>2</sub> are studied in the range 0.25 to 5.0 eV. In an earlier study,<sup>1</sup> to be referred to as I, the infrared phonon and free-electron dispersion properties were measured above and below the transition temperature  $T_t\approx 68^\circ\text{C}$ . The present work extends the spectra to investigate the electron-band transitions both above and below  $T_t$ . In I, it was found that bulk single-crystal VO<sub>2</sub> samples exhibited infrared-active phonon modes for  $T < T_t$  in the energy range  $\hbar\omega = 0.02$  to 0.09 eV. When samples were heated above  $T_t$ , the infrared spectra showed a sudden increase in reflectivity which was fit satisfactorily by assuming the appearance of  $\sim 2 \times 10^{21}$  quasifree electrons per cc. The large dielectric function of these carriers obscured the phonon peaks preventing any infrared optical study of the phonons in the high temperature phase. This large free carrier part of the dielectric function  $\epsilon$  extended up to energies of about 2.0 eV. In the present study which includes bulk crystals and thin-film measurements, free carriers dominate the spectra (for  $T > T_t$ ) below 2.0 eV. However, there is significant structure in the absorption both above and below  $T_t$  at photon energies above 2.5 eV, and additional peaks near 1.0 eV for

<sup>1</sup> A. S. Barker, Jr., H. W. Verleur, and H. J. Guggenheim, *Phys. Rev. Letters* **17**, 1286 (1966).

<sup>2</sup> David Adler and Harvey Brooks, *Phys. Rev.* **155**, 826 (1967).

<sup>3</sup> G. J. Hyland, *J. Phys. C* **1**, 189 (1968).

$T < T_t$ . The positions of these peaks, their polarization dependence, and their temperature dependence are discussed and analyzed in the following sections.

## 2. EXPERIMENTAL METHOD

The optical constants of VO<sub>2</sub> were determined from reflection and transmission studies on bulk single crystals and thin films. The single crystals for these experiments were supplied by H. J. Guggenheim of Bell Laboratories. They were grown by melting V<sub>2</sub>O<sub>5</sub> and passing nitrogen gas over the melt. This causes a slow decomposition of the V<sub>2</sub>O<sub>5</sub> which then recrystallizes as VO<sub>2</sub>. Chemical analysis showed the stoichiometry to be VO<sub>x</sub> with  $x = 2.01 \pm 0.01$ . In the monoclinic, i.e., low-temperature, phase the crystals exhibit a "domain" pattern. The domains differ from each other by a 90° rotation of the  $b_m$  axis about the  $a_m$  axis.<sup>1,4</sup> Figure 1 shows the ion positions and crystal axes. The domain formation limits the possible distinct optical orientations that can be studied in the low-temperature phase to those with the  $E$  vector parallel and perpendicular to the  $a_m$  axis. In the monoclinic phase there are three distinct directions possible for the electric vector  $E$ , namely,  $E \parallel a_m$ ,  $E \parallel c_m$ , and  $E \parallel b_m$ . However, because of domain formation the  $E \parallel a_m$  spectra will be a mixture of the last two. In the high-temperature phase the crystal has the rutile crystal structure, and there are only two distinct polarization directions to be studied. These lie parallel and perpendicular to the  $c_r$  axis. Since the crystallographic transformation at the transition temperature  $T_t$  is approximately<sup>2</sup>

$$a_m \leftrightarrow 2c_r, \quad b_m \leftrightarrow a_r, \quad c_m \leftrightarrow a_r - c_r,$$

the previously mentioned orientations of the  $E$  vector will yield only two distinct optical spectra in the high-temperature phase.

The crystals were oriented and mechanically polished such that the  $a_m(c_r)$  axis was parallel to the major face of the crystals. This generally yielded a polished surface of somewhat less than 1 cm<sup>2</sup>.

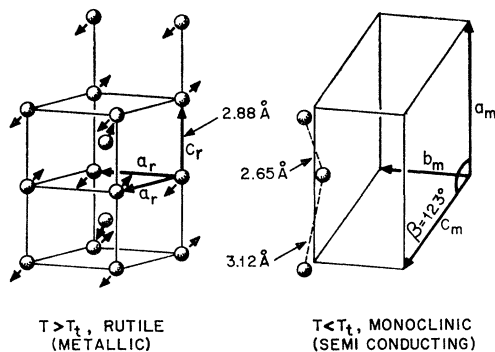


FIG. 1. Illustration of the tetragonal and monoclinic crystal structures of vanadium dioxide.

<sup>4</sup> See, for instance, P. J. Fillingham, J. Appl. Phys. 38, 4823 (1967).

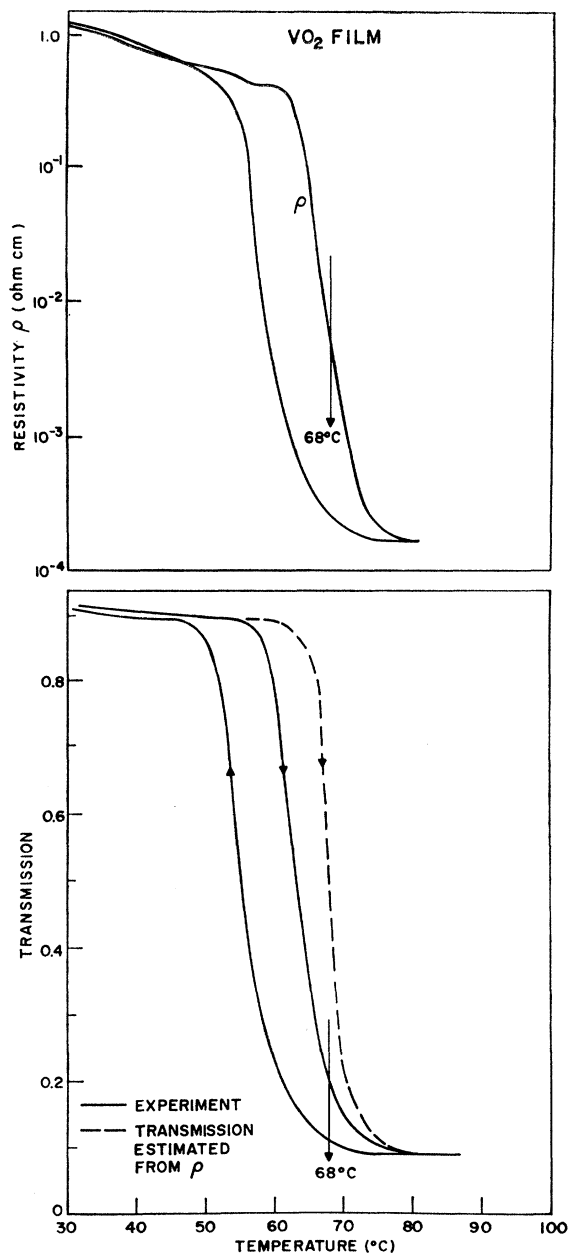


FIG. 2. Temperature dependence of optical transmission at 0.31 eV and resistivity of 1000 Å film of VO<sub>2</sub>.

The thin films of VO<sub>2</sub> used in these experiments were deposited by Hensler.<sup>5</sup> They were deposited on sapphire or rutile (TiO<sub>2</sub>) substrates by reactive sputtering of vanadium in an argon atmosphere with a partial pressure of oxygen.<sup>5</sup> The electrical characteristics of the films are similar to those of bulk VO<sub>2</sub> showing a decrease in resistivity of  $\sim 10^4$  on heating through  $T_t$ . X-ray studies of these films show them to be polycrystalline

<sup>5</sup> E. N. Fuls, D. H. Hensler, and A. R. Ross, Appl. Phys. Letters 10, 199 (1967).

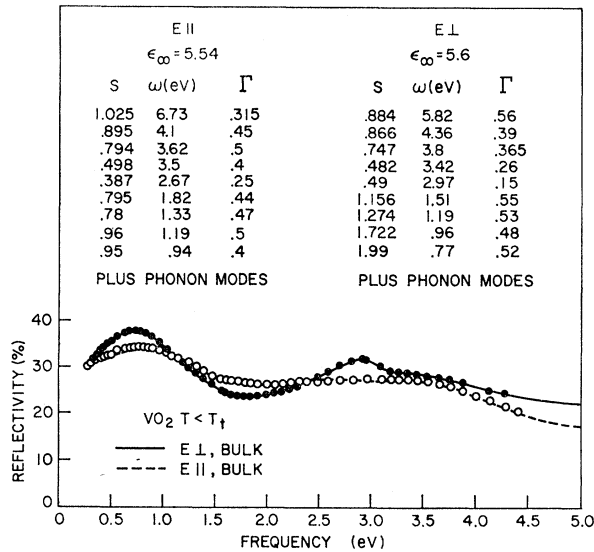


FIG. 3. Reflectivity data and classical oscillator fit for bulk  $\text{VO}_2$  at  $300^\circ\text{K}$ .

$\text{VO}_2$  with a grain size in excess of  $100 \text{ \AA}$ .<sup>5</sup> The crystal-lites can be partially oriented particularly for certain special choices of oriented rutile substrates. Infrared spectra of some films for  $T < T_i$  confirmed the same phonon structure as the bulk crystals studied in I. On heating, the films showed a fairly abrupt transition to free-carrier-dominated behavior. Figure 2 shows the transmission of a  $1000 \text{ \AA}$  film at  $\hbar\omega = 0.31 \text{ eV}$ , well above the fundamental phonon region but below the strong interband transitions. As can be seen there is an abrupt change from transparency to a low-limiting transmission of 0.09 near  $68^\circ\text{C}$ . There is the usual hysteresis effect connected with this first-order transition causing the transmission jump to occur 8 deg lower when the sample is cooled. The resistivity of the film measured simul-

taneously with the transmission in a region adjacent to the infrared beam is also shown in Fig. 2.

The reflection and transmission studies at near normal incidence were made with a single-beam grating spectrometer. The measurements were made point by point with the conventional sample-aluminum-mirror interchange for the reflection studies. The transmission studies of the thin films involved three measurements at each frequency, viz., film plus substrate, substrate only, and air. Because of the relatively poor surface conditions of the bulk samples (cracks and irregularities) as compared to that of the thin films, the reference mirror was formed by evaporating  $2000 \text{ \AA}$  of aluminum directly over half the surface of the bulk crystals. In this manner, surface effects were minimized.

### 3. EXPERIMENTAL RESULTS AND DATA REDUCTION

The reflectivity and transmissivity spectra were determined at two temperatures below  $T_i$ , i.e., at  $90$  and at  $300^\circ\text{K}$ , as well as at a temperature above  $T_i$ , about  $355^\circ\text{K}$ . The experimental results are presented in Figs. 3-6. Figure 3 shows the reflectivity spectra between  $0.25$  and  $5 \text{ eV}$  of a bulk crystal at  $300^\circ\text{K}$ . The two polarizations are distinguished by open and closed circles. The reflectivity spectra of the same crystal for  $T > T_i$  are presented in Fig. 4. The transmissivity and reflectivity spectra of a  $1000 \text{ \AA}$  thin film on a sapphire substrate at room temperature and at  $355^\circ\text{K}$  are presented in Figs. 5 and 6. The transmissivity data are in fact

$$\frac{\text{transmissivity of substrate plus film}}{\text{transmissivity of substrate}},$$

and thus differ somewhat from the actual transmissivity of the film itself. Of course this will be taken into ac-

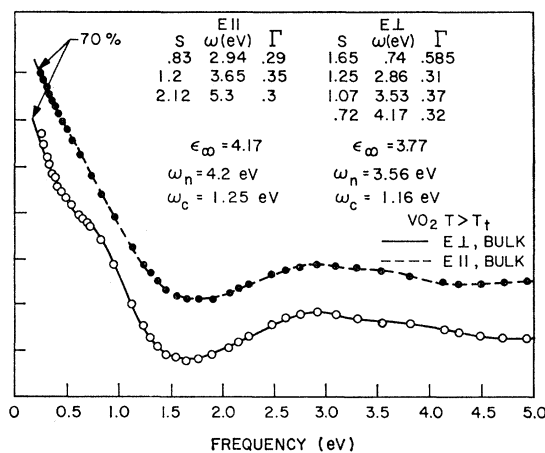


FIG. 4. Reflectivity data and classical oscillator fit for bulk  $\text{VO}_2$  at  $355^\circ\text{K}$ .

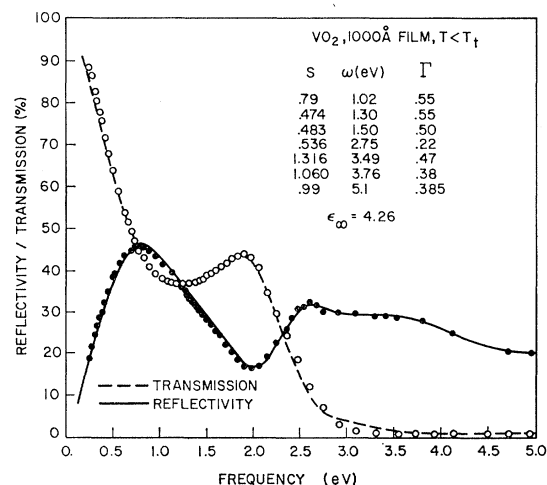


FIG. 5. Reflectivity and transmission data and classical oscillator fits for a  $1000 \text{ \AA}$  film of  $\text{VO}_2$  on sapphire at  $300^\circ\text{K}$ .

count in the analysis. The low-temperature (90°K) results are not shown since these are not significantly different from the room-temperature data.

The reproducibility of the thin-film spectra was good when small variations in thickness between different specimens were taken into account. This was not the case with the spectra of the bulk crystals. While the presence and frequencies of the various peaks in these spectra were not different between the various bulk crystals, the absolute level of the reflectivity varied by as much as 10% between samples. Also, in the high-temperature spectra variations in the plasma edge from one sample to the next by a similar percentage were observed. While the latter could be attributed to different carrier concentrations of the various crystals, the other discrepancies are not easily explained. The most likely explanation is that surface irregularities and cracks are responsible for the variation in absolute level of the reflectivities.

To extract the optical constants from the observed reflectivity and transmissivity spectra a classical oscillator fit was obtained for each spectrum. This method, made very convenient by the adoption of an automatic curve-fitting computer program, has been extensively described elsewhere.<sup>6</sup> It assumes that the complex dielectric constant is given by the following well-known dispersion relation:

$$\epsilon(\omega) = \epsilon_{\infty} - \frac{\omega_n^2}{\omega^2 + i\omega_c\omega} + \sum_{i=1}^n \frac{s_i}{1 - \omega^2/\omega_i^2 - i\Gamma_i\omega/\omega_i}. \quad (1)$$

The first term on the right represents a constant contribution to the real part of the dielectric constant from high-frequency electronic transitions. The second term gives the free-electron contribution to the dielectric constant. Here  $\omega_n = (4\pi n_e e^2/m^*)^{1/2}$  is the carrier density parameter and is related to the plasma frequency, and  $\omega_c = e/\mu_{op} m^*$  is the collision frequency where  $n_e$  is the

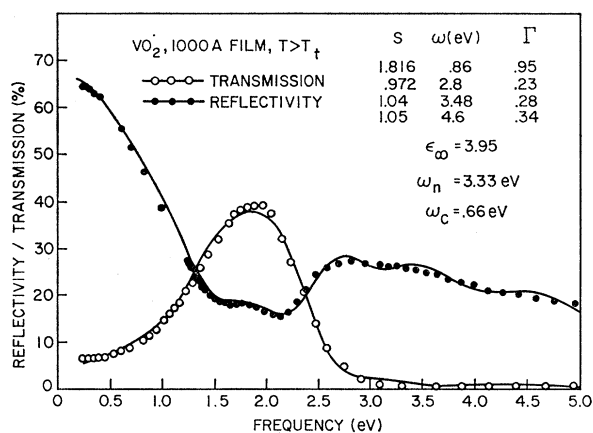


FIG. 6. Reflectivity and transmission data and classical oscillator fits for a 1000 Å film of VO<sub>2</sub> on sapphire at 355°K.

<sup>6</sup> Hans W. Verleur, J. Opt. Soc. Am. (to be published).

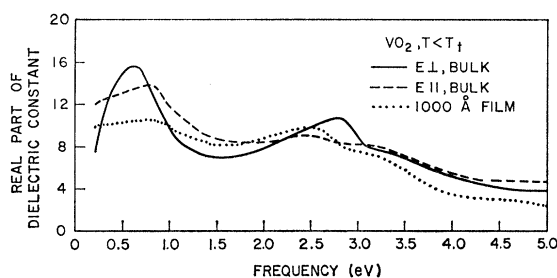


FIG. 7. Real part of dielectric constant  $\epsilon_1$  for VO<sub>2</sub> at 300°K.

number of conduction electrons and  $m^*$  the so-called optical mass of the electrons as defined by Cohen.<sup>7</sup> The third term, which is a sum over Lorentz, or classical, oscillators takes account of the remaining nonconstant contributions to the dielectric constant within the spectral region of interest. These contributions are either due to lattice vibrations or to interband transitions of bound electrons. In this paper the latter are of major interest. While in the case of resonance absorption (lattice vibrations), the strength  $s_i$ , frequency  $\omega_i$ , and linewidth  $\Gamma_i$ , of the  $i$ th oscillator have some physical significance,<sup>6</sup> this in general is not true when Eq. (1) is applied to the spectral region covering interband transitions. Any physical interpretations must be derived from a direct study of the spectra.

The classical oscillator fits to the bulk-reflectivity spectra are represented in Figs. 3 and 4 by the solid and dashed curves, while the oscillator parameters are listed in the figures. In terms of the dielectric constant, defined in Eq. (1), the reflectivity at normal incidence is given by the expression

$$R(\omega) = \left| \frac{\sqrt{\epsilon(\omega)} - 1}{\sqrt{\epsilon(\omega)} + 1} \right|^2. \quad (2)$$

The fitting procedure consists of an initial guess of the number of oscillators and the value of each oscillator parameter. The automatic curve-fitting program, start-

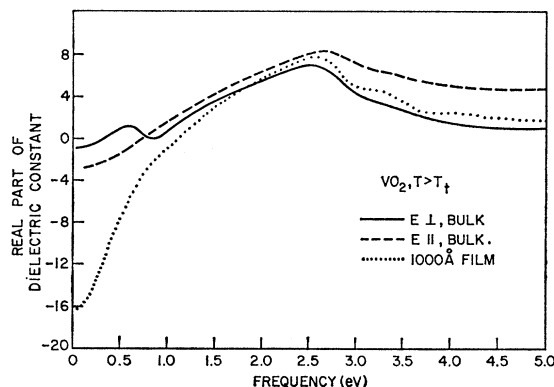


FIG. 8. Real part of dielectric constant  $\epsilon_1$  for VO<sub>2</sub> at 355°K.

<sup>7</sup> M. H. Cohen, Phil. Mag. 3, 762 (1958).

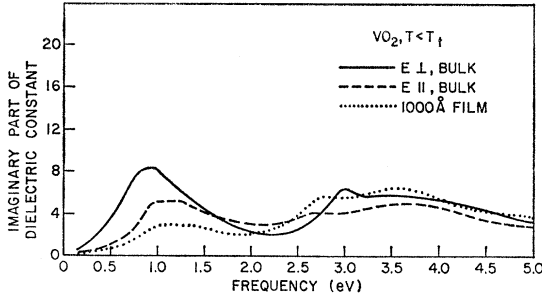


FIG. 9. Imaginary part of dielectric constant  $\epsilon_2$  for  $\text{VO}_2$  at  $300^\circ\text{K}$ .

ing with these initial parameters, which may be quite poor estimates, produces a final set which gives a best fit to the experimental data. The real and imaginary parts of the dielectric constants based on these best fits are given by the solid and dashed curves in Figs. 7-10.

The classical oscillator fits to the transmission and reflection spectra of Figs. 5 and 6 were obtained in a similar manner. If it is assumed that the substrate is sufficiently thick to neglect phase shifts due to multiple reflections within it the transmissivity through film plus substrate is then given by

$$T = T_f T_s, \quad (3)$$

where

$$T_f = n_s \left| \frac{t_f t_s e^{\delta_f}}{1 + r_s r_f e^{2\delta_f}} \right|^2 \quad (4)$$

is the fraction of the incident intensity transmitted into the substrate, and

$$T_s = (1 - R_{sa}) e^{-2\alpha_s d_s} / (1 - R_s R_{sa} e^{-2\alpha_s d_s}) \quad (5)$$

takes account of the additional losses in the substrate. The reflectivity of the two layers is, with the same assumption regarding the substrate,

$$R = R_{fs} + R_{\text{corr}}, \quad (6)$$

where

$$R_{fs} = \frac{r_f + r_s e^{2\delta_f}}{1 + r_f r_s e^{2\delta_f}} \quad (7)$$

is the reflectivity of a film on an infinitely thick substrate and

$$R_{\text{corr}} = T_f^2 R_{sa} e^{-2\alpha_s d_s} / n_s^2 (1 - R_{sa} (1 - R_s) e^{-2\alpha_s d_s}) \quad (8)$$

takes account of the finite thickness of the substrate. The Fresnel coefficients are defined in terms of the refractive indices of film and substrate by

$$t_f = 2 / (1 + n_f - ik_f), \quad (9)$$

$$t_s = 2(n_f - ik_f) / (n_f - ik_f + n_s - ik_s), \quad (10)$$

$$r_f = [1 - (n_f - ik_f)] / [1 + (n_f - ik_f)], \quad (11)$$

$$r_s = [(n_f - ik_f) - (n_s - ik_s)] / [(n_f - ik_f) + (n_s - ik_s)], \quad (12)$$

$$r_{sa} = [(n_s - ik_s) - 1] / [(n_s - ik_s) + 1], \quad (13)$$

and

$$R_s = |r_s|^2, \quad (14)$$

$$R_{sa} = |r_{sa}|^2, \quad (15)$$

$$\delta_f = -2\pi i (n_f - ik_f) d_f / \lambda, \quad (16)$$

$$\alpha_s = -4\pi k_s / \lambda, \quad (17)$$

where  $d_s$  and  $d_f$  are the thicknesses of substrate and film, respectively.

Since  $n$  and  $k$  are defined in terms of the real and imaginary parts of the dielectric constants by

$$n = [\frac{1}{2}(\epsilon_1^2 + \epsilon_2^2) + \epsilon_1]^{1/2} \quad (18)$$

and

$$k = \epsilon_2 / 2n, \quad (19)$$

the fitting procedure starts again from the calculation of Eq. (1) with a set of trial parameters.

The transmission and reflection spectra of the film were fitted simultaneously at each temperature with the same set of oscillators listed in Figs. 5 and 6. Since the solid curves fit the experimental data reasonably well, it may be concluded that the surface conditions of the film, which would effect the reflectivity and transmissivity differently, are quite good. A poor optical surface would not allow a simultaneous fit of the two spectra.

The real and imaginary parts of the dielectric constants based on the classical oscillator fits of Figs. 5 and 6 are given by the dotted curves in Figs. 7-10. Comparing the dielectric constants obtained from the two bulk measurements, it can be seen that besides the anisotropy between the two polarizations there is relatively poor agreement in amplitude between bulk and thin-film results. Yet similar structure appears in both the thin-film and bulk spectra. These two observations together with the already noted poor reproducibility of the bulk measurements seem to suggest that surface effects, not corrected by the deposition of the reference mirror on the crystals, are responsible for the discrepancies. This problem has not been further examined since the energy location and polarization dependence of the structure appearing in these spectra is of primary concern. In Table I the frequencies of the peaks appear-

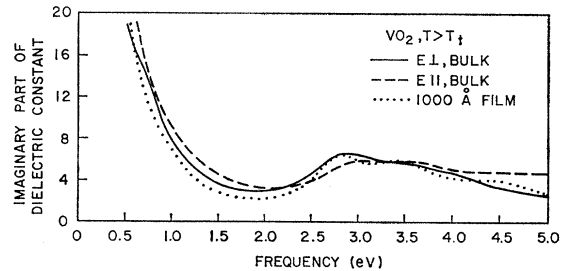


FIG. 10. Imaginary part of dielectric constant  $\epsilon_2$  for  $\text{VO}_2$  at  $355^\circ\text{K}$ .

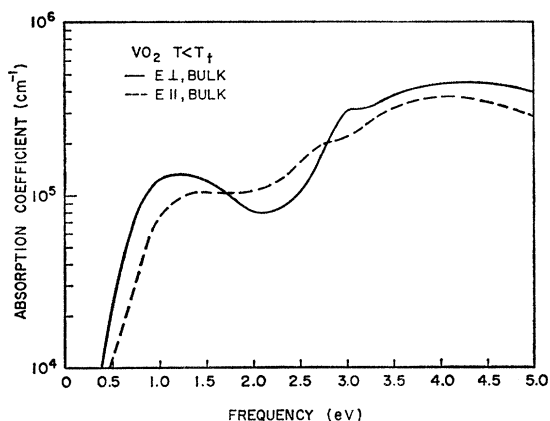
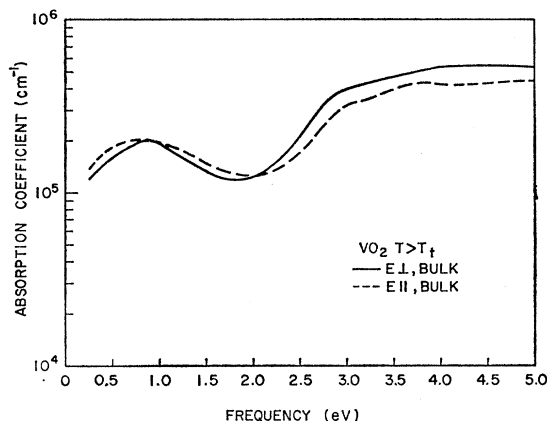
TABLE I. Frequencies of peaks (eV) appearing in the spectra of the imaginary part of the dielectric constant.

$E\parallel a_m$	$T < T_t$		$E\parallel a_m$	$T > T_t$	
	$E\perp a_m$	Film		$E\perp a_m$	Film
1.0	0.85	1.0			
1.3	1.3	1.3		0.75	0.85
2.6	3.0	2.8	3.0	2.9	2.8
3.6	3.7	3.5	3.6	3.6	3.5

ing in the imaginary parts of the dielectric constants at both temperatures are listed. Finally, in Figs. 11 and 12 the absorption coefficients  $\alpha = 4\pi k/\lambda$  for the two polarizations of the bulk crystals are presented.

#### 4. DISCUSSION OF RESULTS

When analyzing and interpreting optical properties of solids, it is often most convenient to do so in terms of a calculated energy-band structure based on the assumptions of one-electron Bloch-wave eigenfunctions and small electron-phonon interactions. Even in solids where such assumptions may be questionable, it has been found that most optical properties can be explained if a reasonably complete band calculation is available and major features such as densities of states and the existence or nonexistence of a band gap can often be predicted. For VO<sub>2</sub> no band calculation is presently available, and there is some question as to whether a Bloch-wave representation is a good approximation at least to the states occupied by the extra *d* electron per vanadium ion. (This point will be discussed in more detail later.) However, there is sufficient information in the literature to permit at least qualitatively both a discussion of the band structure of VO<sub>2</sub> and an interpretation of the optical-absorption properties. The approach that will be taken here will be to first describe a simplified model for the band structure of VO<sub>2</sub> in the high-temperature tetragonal phase. Then the optical data of VO<sub>2</sub> will be discussed in terms of this band structure. In this interpretation the low-temperature mono-

FIG. 11. Absorption coefficient of VO<sub>2</sub> at 300°K.FIG. 12. Absorption coefficient of VO<sub>2</sub> at 355°K.

clinic phase will be treated as a perturbation of the high-temperature phase, but additional consideration will be given to the nature of the states occupied by the extra *d* electron per vanadium ion.

Above 68°C, VO<sub>2</sub> has the rutile (TiO<sub>2</sub>) crystal structure with lattice constants very close to those of rutile. Since vanadium is adjacent to titanium in the periodic table, the energy bands of VO<sub>2</sub> and TiO<sub>2</sub> should also be very similar. Two major effects of replacing Ti with V will be to move the Fermi level to a higher energy to account for the extra *d* electron per vanadium ion, and to modify the relative energy locations of the bands.

Kahn and Leyendecker have calculated the energy-band structure for SrTiO<sub>3</sub> using an LCAO (linear combination of atomic orbitals) method.<sup>8</sup> They obtained very flat bands, especially among the  $\langle 100 \rangle$  directions, with valence bands arising primarily from oxygen *2p* orbitals separated by approximately 3 eV from conduction bands arising primarily from titanium *3d* orbitals. Reasonable agreement of experimental data with this band structure has been reported not only for SrTiO<sub>3</sub>,<sup>9</sup> but also for BaTiO<sub>3</sub><sup>10</sup> and several other perovskite-type materials.<sup>11</sup> In this calculation the electronic structure is dominated by the octahedral configuration of the six oxygen ions surrounding each titanium ion. Rutile has a similar (though somewhat distorted) octahedral arrangement of oxygen ions around the titanium ions, so that it might be expected that a similar band structure is applicable<sup>12</sup> but with modifications in the details of the bands due to the change of crystal symmetry.

<sup>8</sup> A. H. Kahn and A. J. Leyendecker, Phys. Rev. **135**, A1321 (1964).

<sup>9</sup> See, for instance, H. P. R. Frederikse, W. R. Hosler, and W. R. Thurber, Phys. Rev. **143**, A048 (1966); J. F. Schooley, W. R. Hosler, and M. L. Cohen, Phys. Rev. Letters **12**, 474 (1964).

<sup>10</sup> C. N. Berglund and W. S. Baer, Phys. Rev. **157**, 358 (1967); M. DiDomenico, Jr., and S. H. Wemple, *ibid.* (to be published).

<sup>11</sup> S. K. Kurtz, in *Proceedings of the International Meeting on Ferroelectricity* (Prague, 1966), Vol. I, p. 413; A. Frova and P. J. Boddy, Phys. Rev. Letters **16**, 688 (1966); A. Frova and P. J. Boddy, Phys. Rev. **153**, A606 (1967).

<sup>12</sup> A. H. Kahn and A. J. Leyendecker, in *Proceedings of the Seventh International Conference on Semiconductors, Paris, 1964* (Academic Press Inc., New York, 1964), p. 33.

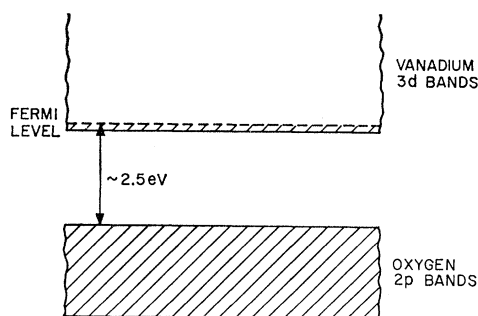


FIG. 13. Energy-band representation for  $\text{VO}_2$ .

For these reasons, in metallic  $\text{VO}_2$  the band scheme will probably be similar to that shown in Fig. 13 with filled oxygen  $2p$  bands separated from partially filled vanadium  $3d$  bands. Similar conclusions have been reached by Goodenough.<sup>13</sup>

In tetragonal  $\text{VO}_2$ , each unit cell of the crystal contains two vanadium ions. As a result, the five  $3d$  orbitals associated with each vanadium ion form ten  $3d$ -type energy bands in the solid. If the  $d$  band with lowest energy were separated by an energy gap from the nine remaining  $d$  bands, the two extra  $d$  electrons associated with the two vanadium ions per unit cell would fill this lowest band completely, thereby producing semiconducting rather than metallic or semimetallic properties. Since semiconducting behavior is not observed in  $\text{VO}_2$  in its tetragonal state, this suggests that the bottom band overlaps at least one of the other nine bands. The degree of overlap is difficult to predict, although presently available experimental data including the low density of free carriers ( $2 \times 10^{21} \text{ cm}^{-3}$ ) measured in I seems more consistent with a model in which the amount of overlap is relatively small.

When  $\text{VO}_2$  is cooled below  $68^\circ\text{C}$ , Andersson<sup>14</sup> found that the crystal structure changes from a tetragonal (rutile) structure to a monoclinic structure. This lower-temperature phase can be looked upon as a slight distortion of the rutile structure, the two major features being a "pairing" of vanadium ions and a doubling of the size of the unit cell (see Fig. 1). Accompanying the phase change is a change in the electronic properties from metallic behavior above  $68^\circ\text{C}$  to semiconductor behavior below  $68^\circ\text{C}$ . Goodenough<sup>15</sup> has postulated that the vanadium ion pairing is due to the formation of homopolar bonds involving the extra  $d$  electron per vanadium ion. The electrons forming these bonds have energy which is separated from an empty antibonding band by a finite energy gap. Adler and Brooks<sup>2</sup> have assumed an energy gap whose energy is dependent on the electronic population of the upper band and on thermodynamic arguments they have shown that such a model is consistent with many of the observed properties of materials which exhibit metal-semiconductor

transitions. Recently, Hyland,<sup>3</sup> applying a theory by Fröhlich,<sup>16</sup> has attributed the low-temperature semiconductor state of  $\text{VO}_2$  to localization of the conduction electrons due to Coulomb correlation. This approach is similar to that suggested by Mott.<sup>17</sup>

Most of the theories described above were developed to explain the electronic properties and the phase transition, and they do not lend themselves readily to the interpretation and discussion of the optical properties of  $\text{VO}_2$  particularly at the higher photon energies. For this reason, a simple band picture will also be applied here to the low-temperature phase of  $\text{VO}_2$ . While such an approach may not be very accurate especially when dealing with those transitions involving the extra  $d$  electron per vanadium ion, in view of the qualitative nature of the interpretation it should provide a reasonable first approximation. In addition, it may be important to show how a simple band picture can be consistent with the metal-semiconductor transition in  $\text{VO}_2$ . However, the optical absorption involving only the extra  $d$  electron per vanadium ion will also be discussed in terms of other models.

The major features of the band structure of  $\text{VO}_2$  in the monoclinic phase should be similar to those in the tetragonal phase. The energy separation between the oxygen  $2p$  bands and the vanadium  $3d$  bands should remain nearly the same, but the doubling of the size of the unit cell will double the number of bands. There will be 20  $3d$  bands made up from the five  $3d$  orbitals of each of the four vanadium ions per unit cell. Since semiconductor behavior is observed, two of these bands must be completely filled and separated from the other eighteen bands by a finite energy gap. In terms of a band picture, this energy gap can arise in two ways, depending on whether the energy shift of the overlapping bands (due to the monoclinic distortion) is larger or smaller than the actual band overlap. In the former case the effects of the monoclinic distortion may be sufficient to remove the overlap completely, thereby leading to semiconductor behavior. This effect is similar to that discussed by Cohen *et al.*<sup>18</sup> In the case where band overlap is large compared to the energy shift resulting from the monoclinic distortion, the energy gap is a consequence of the reduced symmetry and the doubling in size of the unit cell. In either case, the major effect of these band changes on the optical properties will be to replace the free-carrier absorption noted above  $68^\circ\text{C}$  by absorption characteristic of an intrinsic semiconductor below  $68^\circ\text{C}$ . Features of the absorption involving transitions between the oxygen  $2p$  bands and the empty vanadium  $3d$  bands should not be significantly altered, although additional fine structure and slight energy shifts of the peaks might be expected.

<sup>16</sup> H. Fröhlich, in *Proceedings of the Symposium of Ferroelectricity* (Amsterdam, 1967), p. 9.

<sup>17</sup> N. F. Mott, *Proc. Phys. Soc. (London)* **A62**, 416 (1949).

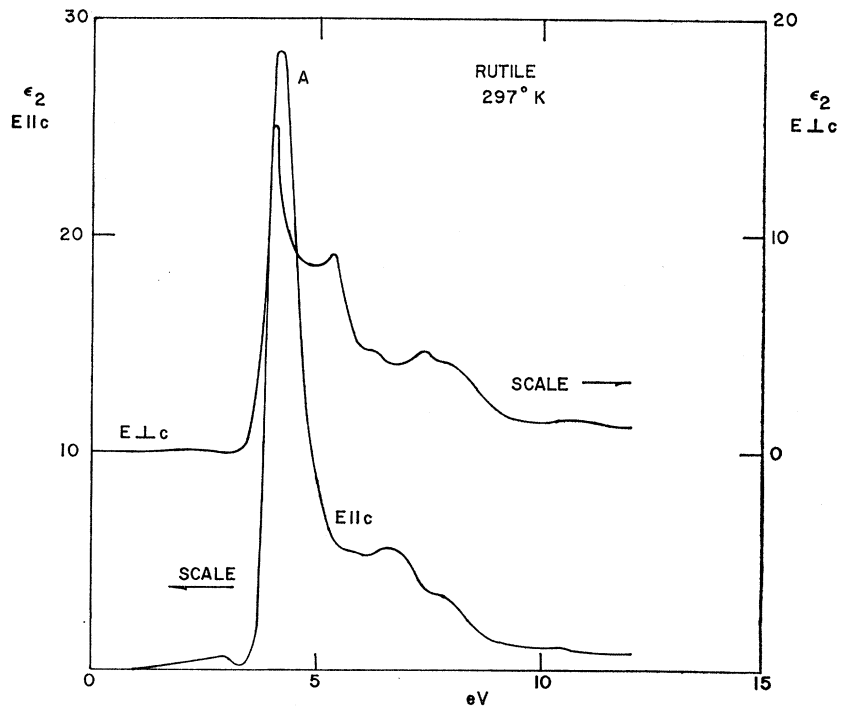
<sup>18</sup> Morrel H. Cohen, L. M. Falicov, and Stuart Golin, *IBM J. Res. Develop.* **8**, 215 (1964).

<sup>13</sup> J. B. Goodenough, *Bull. Soc. Chim. France* **4**, 1200 (1965).

<sup>14</sup> Georg Andersson, *Acta Chem. Scand.* **10**, 623 (1956).

<sup>15</sup> J. B. Goodenough, *Phys. Rev.* **117**, 1442 (1960).

FIG. 14. Imaginary part of the dielectric constant of rutile [reproduced from Cardona and Harbeke (Ref. 19)].



#### A. $T > T_t$

Figure 10 shows the imaginary part of the dielectric constant of VO<sub>2</sub> at temperatures above 68°C. The absorption at photon energies below 2.5 eV is primarily due to free-carrier absorption and will be discussed later. However, the structure at photon energies above 2.5 eV is due to interband transitions, and it is believed that this absorption is due to transitions between the oxygen 2*p* bands and the empty vanadium 3*d* bands. This conclusion is supported by comparing the energy location and polarization dependence of the absorption near 3 eV in VO<sub>2</sub> to the peaks labeled A in the optical properties of rutile<sup>19</sup> (Fig. 14). Photoemission results and a comparison of preliminary reflectivity measurements of VO<sub>2</sub> with rutile using unpolarized light up to photon energies of 12 eV provides additional support to this assignment.<sup>20</sup>

There are two major differences between the peaks located near 3 eV in VO<sub>2</sub> and the peaks labeled A in rutile shown in Fig. 14. First, they are located at approximately 1 eV lower energy in VO<sub>2</sub> and, secondly, the structure in VO<sub>2</sub> is not nearly as sharp or as strong as in TiO<sub>2</sub>. The former is not unusual since it is expected that the energy separation between the titanium 3*d* bands and the oxygen 2*p* bands in rutile will be different than the energy separation between the vanadium 3*d* bands and the oxygen 2*p* bands in VO<sub>2</sub>. How-

ever, the latter is a very striking effect, and there are several possible explanations. Lifetime broadening is probably the least likely explanation not only because of the very large broadening required (of order 1 eV), but also because there has been a significant loss of oscillator strength not expected from a simple lifetime-broadening argument. A more likely explanation of the difference in the magnitude of the absorption is that the final states associated with the absorption peaks in rutile are located in the lowest conduction band. Since the lowest "conduction" band in VO<sub>2</sub> is at least partially occupied by the extra electron per vanadium ion, these transitions would not be allowed in VO<sub>2</sub>.

Cardona and Harbeke<sup>19</sup> have suggested that some of the optical structure up to 10 eV in TiO<sub>2</sub> may arise from exciton effects. Such effects would be expected to give rise to sharp structure near critical points as observed near 4 eV. It is interesting to note that exciton effects would be suppressed due to the screening by the large number of free carriers in VO<sub>2</sub>, and the lack of strong, sharp structure near 3 eV would be expected.

Detailed assignments of the two clearly defined peaks in  $\epsilon_2$  at 2.8 and 3.6 eV cannot presently be made. However, it seems reasonable to conclude from the experimental data that the energy separation between the top of the oxygen 2*p* bands and the vanadium 3*d* bands at the Fermi level is approximately 2.5 eV, and that the two peaks are due to peaks in the joint density of states between these bands.

At photon energies below 2.5 eV,  $\epsilon_2$  exhibits behavior characteristic of free-carrier absorption, but with an

<sup>19</sup> Manuel Cardona and Gunther Harbeke, Phys. Rev. **137**, A1467 (1965).

<sup>20</sup> R. J. Powell, Ph.D. thesis, Stanford University, 1967 (unpublished).



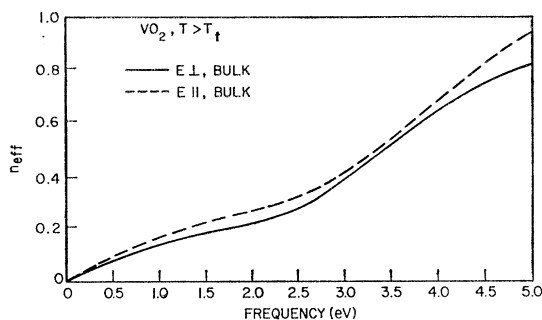


FIG. 15. Effective number of electrons per vanadium ion contributing to the optical absorption in VO<sub>2</sub> at 355°K.

additional shoulder due to an absorption peak centered near 0.7 eV which is most clearly visible for light polarized perpendicular to the  $c$  axis. The carrier density parameter  $\omega_n$  and collision frequency  $\omega_c$  are shown in Fig. 4 and are very similar to those measured and discussed in I.

Philipp and Ehrenreich<sup>21</sup> have expressed the sum rule

$$\mathfrak{N}_{\text{eff}}(\omega_0) = \frac{m}{2\pi^2 N e^2} \int_0^{\omega_0} \omega e_2(\omega) d\omega, \quad (20)$$

where  $\omega$  is the angular frequency of the light,  $m$  is the free-electron mass,  $e$  is the electronic charge,  $N$  is the number of atoms per unit volume, and  $\mathfrak{N}_{\text{eff}}$  is the effective number of electrons per atom contributing to the optical absorption up to a frequency  $\omega_0$ . For application to VO<sub>2</sub> it is more meaningful to define  $N$  as the number of vanadium ions per unit volume, in which case  $\mathfrak{N}_{\text{eff}}$  in Eq. (20) becomes the effective number of electrons per vanadium ion contributing to the absorption.

Figure 15 shows  $\mathfrak{N}_{\text{eff}}$  determined from the optical data of VO<sub>2</sub> in its high-temperature state. Near a photon energy of 2.5 eV there is an abrupt increase in the slope of  $\mathfrak{N}_{\text{eff}}$ . This behavior is consistent with the previously described onset of interband transitions between the oxygen  $2p$  bands and the vanadium  $3d$  bands. If this absorption is subtracted from  $\mathfrak{N}_{\text{eff}}$ , the remainder consists only of the absorption due to the one extra  $d$  electron per vanadium ion. Figure 15 indicates that the photon energy at which that part of  $\mathfrak{N}_{\text{eff}}$  due only to the extra electron per vanadium ion reaches its expected value of unity is considerably larger than 2.5 eV. In fact,  $\mathfrak{N}_{\text{eff}}$  appears to saturate at a value near 0.3 at 2.5 eV. While it is difficult to draw definite conclusions from these observations, the fact that interband transitions within the  $3d$  bands are showing up in the data (the shoulder in  $\epsilon_2$  near 0.7 eV) at photon energies well below 2.5 eV and the low value of  $\mathfrak{N}_{\text{eff}}$  are both qualitatively consistent with a model in which one or more of the  $3d$  bands slightly overlap a lower, nearly filled  $3d$  band.

<sup>21</sup>H. R. Philipp and H. Ehrenreich, Phys. Rev. **129**, 1550 (1963).

### B. $T \approx T_t$

When VO<sub>2</sub> is cooled through the tetragonal-monoclinic phase transition at 68°C, the optical properties particularly in the infrared change markedly. It has been shown previously<sup>1</sup> that most of these changes are due to the onset of strong free-carrier absorption at temperatures above  $T_t$ . It may be of interest to attempt to relate the free-carrier absorption through  $T_t$  to the electrical resistivity.

In Fig. 2 the transmission at  $h\nu=0.31$  eV and the resistivity of a thin VO<sub>2</sub> film similar to that exhibiting the optical properties shown in Figs. 5 and 6 are shown. Since the spectral dependence of the transmission shown in Figs. 5 and 6 indicates that the absorption at  $h\nu=0.31$  eV is dominated by free carriers, it is possible to relate the curves of  $\rho$  and  $T$  in Fig. 2 by the following simplified model. The density of carriers  $n_c$  enters  $\rho$  as  $1/\rho = n_c e^2 \tau / m^*$ , where  $\tau$  is the low-frequency relaxation time.  $n_c$  also enters the dielectric function description (Eq. 1) through the parameter  $\omega_n^2 = 4\pi n_c e^2 / m^*$ . Neglecting changes of  $\tau$  and  $m^*$  with temperature, a relation between  $\omega_n$  and  $\rho$  can be written in the form

$$\omega_n^2 = c/\rho, \quad (21)$$

where  $c$  is a constant. In Fig. 2,  $c$  has been chosen to fit both sets of data at 78°C.

Using the film-transmission formula given earlier, the  $\rho(T)$  data in Fig. 2, and Eq. (21), the transmission at several temperatures for the heating run from 55 to 80°C has been calculated and is plotted as a dashed curve in Fig. 2. This curve falls much more steeply than the observed transmission. The discrepancy probably comes from the infrared beam averaging over many crystalline regions which do not all switch at 68°C. We can picture a few small regions spreading out and finally engulfing the whole sample well above  $T_t$ . (These partial switching effects have been studied by others.<sup>4</sup> The stresses built up in these small regions are probably also responsible at least in part for the hysteresis in the  $\rho$  and transmission curves.) The observed transmission change is then a measure of the film area that has switched through  $T_t$  and is not a measure of the number of carriers present at  $T_t$ . Of course the resistivity itself suffers from the same mixed-phase problem: If a single phase could be studied right up to  $T_t$  the jump in  $\rho$  would have been much steeper. It thus appears impossible with the present samples and techniques to study optical excitation in VO<sub>2</sub> in detail very near  $T_t$ . A similar conclusion on the presence of mixed phases was reached previously.<sup>1</sup> It can, however, be concluded from Fig. 2 that the changes in the optical properties of VO<sub>2</sub> occur with a few degrees of  $T_t$ , and that the optical properties are relatively insensitive to temperature well above or well below  $T_t$ . This conclusion has been further verified by preliminary measurements of VO<sub>2</sub> reflectivity at 90°K. The data are nearly identical to those at room temperature.

### C. $T < T_i$

Figure 9 shows the imaginary part of the dielectric constant for VO<sub>2</sub> measured at 300°K. Above 2.5 eV, structure similar to that observed at 355°K and attributed to transitions between the oxygen 2*p* bands and the empty vanadium 3*d* bands is present. There is a prominent peak for  $E \perp a_m$  located at 3.0 eV, and two less prominent peaks for  $E \parallel a_m$  located at 2.6 and 3.6 eV. Although the polarization dependence of these peaks has changed somewhat compared to the high-temperature data, they too are probably related to the peaks labeled A in rutile (Fig. 14).

At photon energies below 2.5 eV, there is one prominent peak in  $\epsilon_2$  at 0.85 eV for  $E \perp a_m$ , and two peaks near 1.0 and 1.3 eV for  $E \parallel a_m$ . For neither polarization is there a clear-cut onset of absorption as might be expected at a band edge.

There are several ways of examining the optical data of monoclinic VO<sub>2</sub> at photon energies below 2.5 eV, and none are completely satisfactory. If a band scheme is chosen as the basis for interpretation, it can only be concluded at the present time that the absorption peaks near 1.0 eV and their polarization dependences must reflect joint density-of-states peaks and selection rules between the empty and filled vanadium 3*d* bands. However, the spectral dependence of the absorption coefficient below 1 eV shown in Fig. 11 is completely ambiguous as far as identification of the band-gap energy is concerned since it is unlike that expected on a simple band picture. There is no clear threshold. The absorption coefficient increases slowly from a value of approximately 10<sup>3</sup> cm<sup>-1</sup> near 0.2 eV to a value of 10<sup>5</sup> cm<sup>-1</sup> near 1.0 eV. For some samples an additional absorption peak of variable strength was observed near 0.3 eV, which is believed to be due to impurities, imperfections, or departures from stoichiometry. It is possible that similar effects have tended to mask and spread in energy the true band-edge absorption. Such a mechanism would explain the weak temperature dependence of this absorption down to 90°K. If this is true, the energy gap in VO<sub>2</sub> below 68°C is probably greater than 0.5 eV.

Several of the theories presented to explain the semi-conducting state of VO<sub>2</sub> have postulated the existence of a bound state for the extra *d* electron per vanadium ion.<sup>3,16,17</sup> If this model is chosen as a basis for interpretation of the optical data, it may be more reasonable to compare the absorption below 2.5 eV to photo-ionization from a deep impurity level. Referring to the absorption coefficient in Fig. 11, both the spectral dependence and the magnitude normalized by the density of vanadium ions are very similar to that expected from photo-ionization.<sup>22</sup> Using Lucovsky's result that the energy at the absorption peak in photo-ionization from a localized level to a band continuum occurs approxi-

mately at twice the binding energy of the level,<sup>23</sup> the energy gap in VO<sub>2</sub> is approximately 0.6 to 0.7 eV.

One other approach, and intuitively more satisfactory, is to compare the absorption in VO<sub>2</sub> to that of the  $V_k$  center in the alkali halides.<sup>24</sup> In the  $V_k$  center, a hole takes up an orbit on two adjacent halogen ions forming a single ionized halogen "molecule." The formation of this center is accompanied by a lattice distortion, the two halogen ions moving closer to one another, and the complex is only stable at low temperatures. The analogy to the homopolar bond in VO<sub>2</sub> described by Goodenough<sup>15</sup> is striking, and there is a strong similarity in the spectral dependence of the absorption.<sup>24</sup> The only major difference exists in the polarization dependence of the absorption. In the alkali halides, the most prominent absorption is for light polarized in the direction of alignment of the  $V_k$  centers. In VO<sub>2</sub>, the homopolar bonds lie along the rutile *c* axis, so that the dominant absorption might be expected to be for  $E \parallel a_m$ . Although there was some variation in the magnitude of the absorption anisotropy in VO<sub>2</sub>, it was always found that the absorption was larger for  $E \perp a_m$ . However, since the polarization dependence depends on the unknown spatial distribution of the electron wave function, this difference may not be significant.

## 5. CONCLUSIONS

The optical and energy band properties of VO<sub>2</sub> at temperatures above 68°C have been discussed qualitatively in terms of the optical properties and electronic structure of rutile. Although the relatively limited understanding of rutile provides a severe restriction to a detailed analysis of the VO<sub>2</sub> data, several general conclusions are possible. It has been shown that the data are consistent with a model in which filled valence bands, probably associated primarily with the oxygen 2*p* orbitals, are separated by approximately 2.5 eV from partially filled conduction bands. These conduction bands probably arise primarily from the vanadium 3*d* orbitals, and they are occupied only by the extra *d* electron of the vanadium ions. The data indicate that a large fraction of the states in the lowest *d* band are occupied and that this lowest band slightly overlaps one or more partially occupied bands. For this reason it may be more accurate to consider the high-temperature state of VO<sub>2</sub> as a semimetal rather than as a metal.

At temperatures below 68°C, the optical properties indicate that the electrons responsible for the free-carrier absorption at higher temperatures have either become trapped in localized levels or occupy two completely filled bands. In either case, an energy gap of approximately 0.6 eV has formed between the highest

<sup>23</sup> G. Lucovsky, *Solid State Commun.* **3**, 299 (1965).

<sup>24</sup> See, for instance, C. J. Debecq, B. Smaller, and P. H. Yuster, *Phys. Rev.* **111**, 1235 (1958); W. Konziz and T. O. Woodruff, *J. Phys. Chem. Solids* **9**, 70 (1958); R. B. Murray and F. J. Keller, *Phys. Rev.* **137**, A942 (1965).

<sup>22</sup> See, for instance, C. N. Berglund and H. J. Braun, *Phys. Rev.* **164**, 790 (1967).

filled states and the next higher empty conduction band. The major features of the previously identified absorption from the deeper oxygen  $2p$  bands do not change, although relatively small changes in the energy location and polarization dependence of the absorption peaks were observed.

A more detailed comparison of the absorption due to the extra  $d$  electron per vanadium ion at temperatures below  $68^\circ\text{C}$  to that expected on the basis of present theories of the metal-semiconductor transition is inconclusive. Although it is clear that a simple band picture is qualitatively consistent not only with the measured optical properties but also the metal-semiconductor transition, there are indications that such a model may be a considerable oversimplification. In addition, a model based on the assumption that the extra  $d$  electron per vanadium ion is trapped in a local-

ized level has equal qualitative consistency with the data. It is more likely that neither model is completely correct. Since the extra  $d$  electron per vanadium ion is largely responsible for the crystal forces which result in the distorted, monoclinic structure at temperatures below  $68^\circ\text{C}$ , effects in optical absorption similar to those observed in the  $F$  and  $V_k$  centers of the alkali halides are expected to occur.

#### ACKNOWLEDGMENTS

The authors wish to thank H. J. Guggenheim and D. H. Hensler for supplying the  $\text{VO}_2$  crystals and films studied in this work, and G. E. Mahoney for making many of the measurements. Helpful comments and suggestions from G. E. Smith and J. Brews, and very useful discussions about the band structure of  $\text{VO}_2$  with L. Mattheiss are also gratefully acknowledged.

## Electroreflectance Studies of InAs, GaAs, and (Ga,In)As Alloys\*

E. W. WILLIAMS†

*Royal Radar Establishment, Malvern, Worcestershire, England*

AND

VICTOR REHN

*Michelson Laboratory, China Lake, California 93555*

(Received 2 October 1967; revised manuscript received 5 April 1968)

The technique of electroreflectance was applied to the study of epitaxial (Ga, In)As alloys. Two experimental methods were used and their relative merits are discussed. The  $\Gamma_{15}-\Gamma_1$  and  $\Lambda_3-\Lambda_1$  transitions and their spin-orbit splittings were investigated as functions of alloy composition. The spin-orbit splitting at  $k=0$  for InAs at room temperature was measured directly as  $0.446 \pm 0.008$  eV. The electroreflectance linewidth changes by a factor of 4 for the  $\Gamma_{15}-\Gamma_1$  series between InAs and GaAs. The broadening is discussed in terms of mechanisms such as field inhomogeneity and light-hole lifetime for the InAs-rich alloys. The deviations from a linear concentration dependence that were observed for all of the energy gaps were almost all identical and were related to the virtual-crystal model. Transitions below the fundamental gap were correlated with impurities by the use of photoluminescence measurements on the same samples.

### I. INTRODUCTION

THE energy-band structures of GaAs and InAs have been calculated theoretically<sup>1,2</sup> and a large number of experimental results have yielded band-structure parameters. Of the experimental techniques available, only optical techniques allow the experimenter to study a wide range of interband energy, and

conventional normal-incidence reflectivity and optical-absorption measurements have been made on these materials previously. Woolley and Blazey<sup>3</sup> studied the  $\Lambda_3-\Lambda_1$ ,  $\Gamma_{15a}-\Gamma_{15c}$ , and  $X_5-X_1$  interband transitions by normal-incidence reflectance in polycrystalline samples of (Ga,In)As alloys and concluded that the energies of these transitions vary linearly with composition. Jones<sup>4</sup> subsequently used the same technique and found that the  $\Lambda_3-\Lambda_1$  transition energy showed a nonlinear dependence on composition at the InAs end of the alloy series. Optical-absorption studies of the fundamental absorption region in these alloys have been

\* A preliminary version of this paper was given at the New York A. P. S. Meeting: Bull. Am. Phys. Soc. **12**, 101 (1967).

† The experimental work described here was performed while this author was with Texas Instruments Incorporated, Dallas, Tex. 75222.

<sup>1</sup> Marvin L. Cohen and T. K. Bergstresser, Phys. Rev. **141**, 789 (1966).

<sup>2</sup> F. H. Pollak, C. W. Higginbotham, and M. Cardona, J. Phys. Soc. Japan Suppl. **21**, 20 (1966).

<sup>3</sup> J. C. Woolley and K. W. Blazey, J. Phys. Chem. Solids **25**, 713 (1964).

<sup>4</sup> C. E. Jones, Appl. Spectry. **20**, 161 (1966).